

Range optimized theory of electron liquids with application to the homogeneous gas

James P. Donley*

*Department of Materials and Metallurgical Engineering,
New Mexico Institute of Mining and Technology, Socorro, NM, 87801[†]*

(Dated: September 11, 2021)

A simple optimization scheme is used to compute the density-density response function of an electron liquid. Higher order terms in the perturbation expansion beyond the random phase approximation are summed approximately by enforcing the constraint that the spin density pair correlation functions be positive. The theory is applied to the 3-D homogeneous electron gas at zero temperature. Quantitative comparison is made with previous theory and data from quantum Monte Carlo simulation. When thermodynamic consistency is enforced on the compressibility, agreement with the available simulation data is very good for the entire paramagnetic region, from weakly to strongly correlated densities. In this case, the accuracy of the theory is comparable to or better than the best of previous theory, including the full GW approximation. In addition, it is found that the spin susceptibility diverges at a lower density ($r_s \approx 107$) than the current estimate for the liquid-solid transition. Application of the theory to inhomogeneous electron liquids is discussed.

PACS numbers: 71.10.Ca, 71.10.-w, 71.10.Hf

I. INTRODUCTION

In many practical calculations of electronic structure, such as for semiconductors and molecules, the density-density response function χ plays a central role. The popular Kohn-Sham electronic density functional theory (DFT)[1–3], and Hedin’s “GW” approximation (GWA) of many-body perturbation theory[4, 5] are two such methods that use χ .

In DFT, χ is an important ingredient in the exchange-correlation functional, E_{xc} , which is the main object for approximations in the theory.[2] The workhorse local density approximation (LDA) and its generalizations avoid explicitly estimating χ for the inhomogeneous liquid. Instead, they approximate E_{xc} by relying on knowing the correlations of a simpler system, the homogeneous electron gas, i.e., jellium.[6] The correlations of this latter system have been computed accurately using theory and quantum Monte Carlo (QMC) simulation.[7] While being very accurate for the electron structure of molecules and electron density of many systems, DFT-LDA and its variants have the limitation of not being able to describe accurately band gaps, nor London dispersion (i.e., van der Waals) interactions very well.[2] The former is crucial to understanding the properties of semiconductors, while the latter is important to understanding weakly bonded systems, such as water. A recent branch of DFT uses the adiabatic-connection fluctuation-dissipation form for the correlation energy, which is the troublesome part of E_{xc} . In this branch there is much current interest in the use of the random phase approximation (RPA) for χ . [8] Unlike the LDA, this DFT-RPA does predict reasonable band gaps for many solids,[9] and, with some extra effort, reasonable London dispersion interactions between

atoms.[10, 11]

In GWA, χ enters through the screened potential W to compute ultimately the one-particle Green’s function, G , from which the band structure is extracted.[4, 6] In perturbative calculations around a DFT reference state, known as “one-shot GW,” χ is almost always taken to have a simple RPA form. In the full version of GWA, χ is computed in a self-consistent loop along with G . Being able to predict accurate band structure for many solids, GWA has rapidly become one of the main methods for computing the electronic structure of crystalline materials.[12, 13] A drawback to this approach though is that the full, self-consistent solution often does not improve the predictions of the theory, and can make it worse.[14] Application of the GWA to jellium has shown that the main weakness is the expression for χ obtained from G . [14]

For both approaches then, a better way to compute χ would be very desired. In this paper, a simple scheme called range optimization is described that goes beyond the RPA for χ to accomplish this task. Range optimization was originally used to improve the RPA theory of classical molecules. This “range-optimized” RPA (RO-RPA) theory was able to describe very well the equilibrium structure and thermodynamics of strongly charged polyelectrolyte solutions.[15–17] It has also been applied successfully to the study of the hydrated electron.[18] Given that a number of weaknesses of the GWA became apparent only after the full version had been implemented for jellium, it is important for the theory here to be analyzed first for that system. This is the intent of the present paper. As will be shown below, the scheme applied to jellium greatly improves the predictions of the theory over the basic RPA. A new algorithm to implement range optimization, valid for inhomogeneous liquids, is also described here.

* jdonley@valence4.com

[†] Also at Valence4 Technologies, Arlington, VA 22202

II. THEORY

Let the analysis be confined to a homogeneous electron gas, i.e., jellium, in 3-D at zero temperature in the paramagnetic phase. As a reminder, jellium has a balancing background of positive charge that is uniform and rigid.[6, 19]

The theory here is centered around the time-ordered, spin density-density response function (or spin polarization propagator), $\chi_{ij}(x, x')$, where i and j label the spin (\uparrow and \downarrow), and $x \equiv \{\mathbf{r}, t\}$, with \mathbf{r} being the position and t the time. It is defined as:

$$\chi_{ij}(x, x') = \frac{1}{i\hbar} \frac{\langle \Psi_0 | T[\delta \hat{n}_i(x) \delta \hat{n}_j(x')] | \Psi_0 \rangle}{\langle \Psi_0 | \Psi_0 \rangle}. \quad (\text{II.1})$$

Here, $|\Psi_0\rangle$ is the system ground state, and T denotes the time ordered product. Also,

$$\delta \hat{n}_i(x) = \hat{n}_i(x) - \langle \hat{n}_i(x) \rangle, \quad (\text{II.2})$$

where $\hat{n}_i(x)$ is the number density operator in the Heisenberg representation for spin i electrons at point x , [19] and $\langle \hat{n}_i(x) \rangle$ denotes its ground state average. For the paramagnetic phase, $\langle \hat{n}_\uparrow(x) \rangle = \langle \hat{n}_\downarrow(x) \rangle = n/2$, where n is the average electron density.

Jellium is translationally invariant and χ is symmetric with respect to $x \leftrightarrow x'$, so $\chi_{ij}(x, x') \rightarrow \chi_{ij}(r, \tau)$, where $r = |\mathbf{r} - \mathbf{r}'|$ and $\tau = t - t'$. For this case, it is helpful to work with the dual Fourier transform, $\chi_{ij}(k, \omega)$, $k = |\mathbf{k}|$ being the wavevector and ω the frequency.

A number of useful quantities can be obtained from $\chi_{ij}(k, \omega)$. [6] First is the system compressibility K :

$$\frac{K_0}{K} = -N(0) \lim_{k \rightarrow 0} \left[\frac{1}{\chi(k, 0)} + v(k) \right], \quad (\text{II.3})$$

where $\chi(k, \omega) = \sum_{ij} \chi_{ij}(k, \omega)$ is the total density-density response function, and $N(0) = mk_F/(\pi^2 \hbar^2)$, with m being the electron mass, and $k_F = (3\pi^2 n)^{1/3}$ being the Fermi wavevector. [6] Also, K_0 is the compressibility of the non-interacting gas, and $v(k)$ is the Fourier transform of the electron-electron Coulomb potential, $v(r) = e^2/r$, with e being the electron charge. Second is the spin susceptibility χ_S :

$$\frac{\chi_P}{\chi_S} = -N(0) \lim_{k \rightarrow 0} \left[\frac{1}{2(\chi_{\uparrow\uparrow}(k, 0) - \chi_{\uparrow\downarrow}(k, 0))} \right], \quad (\text{II.4})$$

where χ_P is the spin susceptibility of the non-interacting gas. Third are the partial static structure factors:

$$S_{ij}(k) = \frac{2i\hbar}{\pi n} \int_0^\infty d\omega \chi_{ij}(k, \omega), \quad (\text{II.5})$$

which are real, and have exploited that $\chi_{ij}(k, \omega)$ is symmetric about $\omega = 0$. Fourth are the spin-spin pair correlation (or radial distribution) functions:

$$g_{ij}(r) = 1 + \frac{2}{n} \int \frac{d\mathbf{k}}{(2\pi)^3} [S_{ij}(k) - \delta_{ij}] \exp(i\mathbf{k} \cdot \mathbf{r}), \quad (\text{II.6})$$

where δ_{ij} is the Kronecker delta. The pair correlation function $g_{ij}(r)$ is proportional to the equilibrium probability density of there being an electron of spin j a distance r from one with spin i at the same time. As a density, $g_{ij}(r)$ is strictly positive for all r . Last, the correlation energy E_{corr} can be obtained from $S_{ij}(k)$. [19] Two expressions for E_{corr} were used and they are given in Sec. III below.

Define the matrix inverse of $\chi_{ij}(k, \omega)$ by $\sum_s \chi_{is}(k, \omega) \chi_{sj}^{-1}(k, \omega) = \delta_{ij}$. This inverse can be represented exactly as:

$$\chi_{ij}^{-1}(k, \omega) = \tilde{\chi}_{ij}^{-1}(k, \omega) - v_{ij}(k), \quad (\text{II.7})$$

where $v_{ij}(k) = v(k)$, and $\tilde{\chi}_{ij}(k, \omega)$ is the proper spin density-density response function (or proper spin polarization propagator). [6, 19] It is helpful to rewrite Eq.(II.7) as:

$$\chi_{ij}^{-1}(k, \omega) = \chi_{0ij}^{-1}(k, \omega) - v_{ij}(k) - u_{ij}(k, \omega), \quad (\text{II.8})$$

where $u_{ij}(k, \omega) = \chi_{0ij}^{-1}(k, \omega) - \tilde{\chi}_{ij}^{-1}(k, \omega)$ and $\chi_{0ij}(k, \omega) = \delta_{ij} \chi_0(k, \omega)/2$, with $\chi_0(k, \omega)$ being the total density-density response function of the non-interacting gas, i.e., the Lindhard function. This Lindhard function can be computed analytically. [19]

Setting $u_{ij}(k, \omega)$ to zero reduces Eq.(II.8) to the familiar RPA expression for χ_{ij} . [6] As is well known, the RPA tends to work well if the interactions are weak. However, for strongly interacting systems it works less well, causing, for example, the pair correlation functions $g_{ij}(r)$ to be (very) negative at small r .

More recent research on jellium has steadily improved upon the RPA. Almost all of these theories have worked with the one-component expression for the total density-density response function, $\chi(k, \omega)$, by developing accurate approximations to the static and dynamic local field factors, $G_+(k)$ and $G_+(k, \omega)$, respectively. These are defined by:

$$\chi^{-1}(k, \omega) = \chi_0^{-1}(k, \omega) - v(k)[1 - G_+], \quad (\text{II.9})$$

where G_+ denotes $G_+(k)$ or $G_+(k, \omega)$. In this manner, the one-component optimized potential, $u = -vG_+$.

The best of these theories now agree with QMC simulation data for the paramagnetic state for the correlation energy E_{corr} within a few percent for the density range of most metals, $2 < r_s < 6$. [7, 20] Here, $r_s = r_0/a_0 = 1/(\alpha k_F a_0)$, where $r_0 = (3/(4\pi n))^{1/3}$ is the average distance between electrons, a_0 is the Bohr radius, and $\alpha = (4/(9\pi))^{1/3}$. A limitation of these theories though is that they usually apply only to the paramagnetic, i.e., zero polarization state. This local field factor approach can be extended to examine partially polarized states, and thus give information about the jellium phase diagram. [21] However, the cost is an increase in the complexity of the theory. As such, a different path will be taken here.

To go beyond the RPA for the multi-component model, Eq.(II.8), the range optimization scheme will be used.

This scheme has been described in detail elsewhere,[15, 16] but a summary is given here.

The aim is to approximate the higher order terms embodied in $u_{ij}(k, \omega)$ in some manner. First, let $u_{ij}(k, \omega)$ be independent of frequency ω . This approximation is not necessary, but is a sensible one for computing the static equilibrium properties of the gas, such as $g_{ij}(r)$ and E_{corr} . Next, let $u_{ij}(k)$ be real. This follows the common assumption that the static local field factor $G_+(k)$ is dominated by its real part.[6] In this manner, the inverse Fourier transform of $u_{ij}(k)$, $u_{ij}(r)$, can be viewed as a short-ranged attractive potential that counteracts the strong electron-electron Coulomb repulsion in $v(r)$ at small r . What then is $u_{ij}(r)$?

Now, the RPA works well at high density, $r_s < 1$, where the kinetic energy and exchange interactions dominate the Coulomb repulsion. At low density, $r_s \gg 1$, where the RPA breaks down, the electron-electron Coulomb repulsion causes $g_{ij}(r)$ to be essentially zero out to some range σ_{ij} (see Figure 1). Notice though that if $g_{ij}(r)$ were zero, it makes little difference to the electrons that the repulsion at that distance were infinite as opposed to just very large. As such, replace the Coulomb potential with a hard-core one for distances $r < \sigma_{ij}$. While the RPA fails for hard-core potentials naturally, methods developed in the classical theory of liquids have found ways to overcome this problem.[22] One is the mean spherical approximation (MSA) closure.[23]

Applied to jellium, the MSA states that if σ_{ij} is the range of the hard-core potential between electrons of spin i and j , then $g_{ij}(r)$ is zero inside this range. But since $g_{ij}(r)$ is zero inside, the equations relating $u_{ij}(r)$ to $g_{ij}(r)$ can be used to determine $u_{ij}(r)$ inside. That is, $u_{ij}(r)$ takes whatever form is needed to ensure that $g_{ij}(r)$ is zero inside the core. The closure is summarized as:

$$\begin{aligned} g_{ij}(r) &= 0, \quad r < \sigma_{ij}, \\ u_{ij}(r) &= 0, \quad r > \sigma_{ij}. \end{aligned} \quad (\text{II.10})$$

This closure, along with Eqs. (II.5), (II.6) and (II.8), form a closed set of equations for $g_{ij}(r)$ and $u_{ij}(r)$, assuming the σ_{ij} are known. The last step is to optimize the range, σ_{ij} , by letting it have the smallest value such that $g_{ij}(r)$ is positive for all r . Since the theory will now work properly for low and high densities, it presumably will work well for intermediate densities as well. This set of self-consistent equations will be referred to as RO-RPA theory.

There are at least two ways to compute the compressibility: by the structure route using $\chi(k, 0)$ in Eq.(II.3), and by the energy route using an expression for the total energy[6]. Since the RO-RPA theory is approximate, the structure and energy routes will not give the same value for K . It is well known though that enforcing consistency between these two routes, i.e., enforcing the “sum rule”, can improve a theory, often greatly.[24] This thermodynamic consistency can be attained under range optimization by noticing that $g_{ij}(r)$ need not be set to zero inside the core. Instead, the minimum of $g_{ij}(r)$ could

have a non-zero value, g_0 . The MSA closure can then be generalized to:

$$\begin{aligned} g_{ij}(r) &= g_0, \quad r < \sigma_{ij}, \\ u_{ij}(r) &= 0, \quad r > \sigma_{ij}, \end{aligned} \quad (\text{II.11})$$

where the value of g_0 is determined by enforcing the sum rule on the compressibility. This extra condition, along with the RO-RPA equations above, will be referred to as “thermodynamically consistent” RO-RPA (TCRO-RPA) theory.

III. NUMERICAL SOLUTION

All theories were solved numerically as follows. Functions of r or k were solved on a grid of N_r points with spacing Δr or $\Delta k = \pi/(N_r \Delta r)$, respectively. Unless stated otherwise, N_r and Δr were set to 2^{11} and $0.05/k_F$, respectively. To compute the static structure factor $S_{ij}(k)$, the integration of $\chi_{ij}(k, \omega)$ over ω given by Eq.(II.5) was performed along the positive real axis. It is well known that along the real axis, a contribution to $S_{ij}(k)$ from the plasmon mode must be accounted for[6, 25] and that was done. As a check though, the integration was also performed along the positive imaginary axis.[4, 25] In either case, the integral over frequency was evaluated using Romberg integration[26] with the relative error tolerance being 10^{-6} and 10^{-9} for the real and imaginary axis cases, respectively.

Once $S_{ij}(k)$ was computed, the integral over k in Eq.(II.6) was evaluated by inverse Fourier transform to obtain $g_{ij}(r)$. As a check on the accuracy, the RPA values for $g_{ij}(0)$ were computed. It was found that unlike the correlation energy, E_{corr} , $g_{ij}(0)$ was sensitive to the grid spacing, but setting $N_r = 2^{16}$ and $\Delta r = 0.05/(32k_F)$ gave convergent RPA values of $g_{ij}(0)$ within 0.1%.[27] The grid spacing did not affect greatly any other quantity, though for increased accuracy in determining the density at which the spin susceptibility χ_S diverged, N_r and Δr were set to 2^{13} and $0.0125/k_F$, respectively, for $r_s \geq 70$.

A new algorithm was used to implement range optimization. This new algorithm has two advantages over the one used in past work[15–18]: it is straightforward to apply to inhomogeneous liquids, and is more efficient even for jellium. It is as follows: 1) An initial guess is made for the optimized potentials $u_{ij}(r)$, which could be zero. 2) With the $u_{ij}(r)$, the theory is solved as described above for the pair correlation functions $g_{ij}(r)$. 3) The difference $\Delta g_{ij}(r) = g_{ij}(r) - g_0$ is computed for all r , where $g_0 = 0$ for standard range optimization. 4) As a variation on Picard iteration[22], the change in the value of the optimized potential is set to $\alpha \Delta g_{ij}(r)$, with the mixing parameter $\alpha \leq 0.25$. 5) Since the optimized potential is an attractive potential, its new value for each r is checked to determine if it is greater than zero; if so, it is set to zero. 6) The difference between the new and old values is checked to determine if the potential has

converged; if not, the steps starting at 2) are repeated until convergence is obtained. Here, the relative error tolerance on each point of $u_{ij}(r)$ was 10^{-4} , although in some cases it was reduced to 10^{-5} as a check.

Note that in this algorithm the optimized ranges, σ_{ij} , are not considered explicitly. Instead, the algorithm relies on knowing only the value of the pair correlation function, g_{ij} , to obtain a refined guess for the optimized potential, u_{ij} , at the same point. In that way, the above algorithm can be used for inhomogeneous liquids by the mere replacement of $g_{ij}(r)$ and $u_{ij}(r)$ with $g_{ij}(\mathbf{r}_1, \mathbf{r}_2)$ and $u_{ij}(\mathbf{r}_1, \mathbf{r}_2)$, respectively, and then using the inhomogeneous analog of Eq.(II.8).[28]

For all theories except TCRO-RPA the correlation energy was computed in the usual manner as a charging integral over the coupling constant e^2 , i.e., via the adiabatic-connection fluctuation-dissipation theorem.[19] Define $\epsilon_c = 2a_0 E_{corr}/(Ne^2)$ as a scaled correlation energy per particle (in units of Rydbergs), with N being total number of electrons. Then this energy equation is:

$$\epsilon_c(r_s) = \frac{4\pi}{\alpha r_s} \int_0^1 d\lambda w(\lambda), \quad (\text{III.1})$$

where

$$w(\lambda) = \frac{1}{2\pi^2 k_F} \int_0^\infty dk [S(k, \lambda) - S(k, 0)]. \quad (\text{III.2})$$

Here, $S(k, \lambda) = 1/2 \sum_{ij} S_{ij}(k, \lambda)$ is the total structure factor for a gas with electron-electron potential $\lambda v(r)$. The integral over k , Eq.(III.2), was computed via quadrature. The charging integral, Eq.(III.1), was computed using Romberg integration with an error tolerance of 10^{-4} .

Enforcing thermodynamic consistency for the TCRO-RPA theory was done as follows. First, for a given value of r_s , a value for g_0 was guessed. Then the optimized potentials, $u_{ij}(r)$, were computed in the same manner as for the RO-RPA. Next, the compressibility was computed using the structure route formula, Eq.(II.3). For the compressibility via the energy route, its value was computed initially using the Perdew-Wang fit for the correlation energy E_{corr} ,[29] and an expression relating the total energy to the compressibility.[6] The change in the value of g_0 was set proportional to the difference between values of K_0/K from these two routes. With this new g_0 , steps 2)-6) above were repeated, and this iteration was continued until the value of g_0 converged. This procedure was repeated to obtain $\chi_{ij}(k, \omega)$ on a grid for $0 \leq r_s \leq 11$ (see below) with spacing $\Delta r_s = 0.1$.

These density-density response functions were then used to compute the correlation energy over this range. The representation of E_{corr} expressed as an integral over r_s was used:[30, 31]

$$\epsilon_c(r_s) = \epsilon_c^{rpa}(r_s) - \frac{4}{\pi \alpha r_s^2} \int_0^{r_s} dx \Delta\gamma(x), \quad (\text{III.3})$$

where

$$\Delta\gamma(r_s) = -\frac{1}{2k_F} \int_0^\infty dk [S(k, r_s) - S_{rpa}(k, r_s)]. \quad (\text{III.4})$$

Here, $\epsilon_c^{rpa}(r_s)$ and $S_{rpa}(k, r_s)$ are the RPA values for the correlation energy and total structure factor, respectively, at mean separation r_s . An accurate interpolation formula for ϵ_c^{rpa} due to Perdew-Wang[29] was used here.

The integral, Eq.(III.4), for $\Delta\gamma(r_s)$ was computed for each r_s in the same manner as for Eq.(III.2). The energy route expression for the compressibility consists of derivatives of ϵ_c with respect to r_s . To minimize errors then, this set of $\Delta\gamma$ values was then fit to an n th degree polynomial in r_s . Degree $n = 11$ was found to give a sufficiently accurate fit ($n = 9$ worked almost as well). With this functional form, Eq.(III.3) was evaluated analytically. The self-consistent theory for g_0 was then solved again, with the new and old values for ϵ_c being used to compute the energy route K with a mixture of 1:1 old to new. After new density-density response functions, $\chi_{ij}(k, \omega)$ were computed, the procedure to compute new values for ϵ_c was repeated. It was found that the fitted values for K had converged to within 10^{-3} (10^{-5} for ϵ_c) for $r_s \leq 10$ after seven iterations.

At $r_s \approx 0$, $g_0 \approx 0$ naturally, then g_0 rose to a maximum of 0.177 at $r_s \approx 1.7$, and then gradually dropped to zero again at $r_s \approx 10.8$. When the positivity constraint on $g_{ij}(r)$ was relaxed, g_0 became slightly negative as r_s increased beyond 10.8. Since this positivity constraint on $g_{ij}(r)$ is more important than enforcing a sum rule, $r_s \approx 10.8$ is then the limit of the usefulness of enforcing thermodynamic consistency on the compressibility. However, it will be shown below that since the RO-RPA is most accurate at low density, this limit is not regarded as important.

For comparison, some results of the theories of Singwi-Tosi-Land-Sjölander (STLS),[30] and Utsumi and Ichimaru (UI) [31] will also be shown. The UI theory is considered accurate for the short range behavior of the pair correlation function at metallic densities.[7] The STLS theory is considered accurate for the correlation energy and almost as accurate as UI for the pair correlation function, but is also straightforward to implement. The theory has also been generalized to apply to inhomogeneous liquids in atoms and ions.[32] The STLS theory was solved for the total structure factor $S(k)$ in a similar manner to that of $S_{ij}(k)$ for the RO-RPA. Once $S(k)$ was determined self-consistently, the spin-averaged $g(r) = 1/4 \sum_{ij} g_{ij}(r)$ was obtained by inverse Fourier transform using the analog of Eq.(II.6). The UI theory was solved in the same manner as the RPA, but with $v(k) \rightarrow v(k)(1 - G_+(k))$. Values for the static local field factor $G_+(k)$ were interpolated from data presented in Table I of [31].

IV. RESULTS

Unless noted otherwise, all RO-RPA results given here will be for the multi-component version described in Sec.II above. Results of the one- and multi-component versions of the RPA are the same for the quantities ex-

amined here.

Figure 1 shows results for the spin-averaged pair correlation function, $g(r)$, for various densities. As a comparison, QMC simulation data of Ceperley and co-workers is also shown.[33, 34] As can be seen, the predictions of the RO-RPA are much improved over the RPA, with the RO-RPA outperforming, as expected, the STLS theory at very low density, $r_s = 50$. For $r_s = 2$, the contact value, $g(0) = 0.176$ and 0.175 for the UI and TCRO-RPA theories, respectively, which are 10% smaller than the simulation value. For $r_s = 10$, the thermodynamically consistent value of g_0 was close to zero. Consequently, the TCRO-RPA prediction for $g(r)$ (not shown) is almost the same as the RO-RPA for this density (and lower densities). Holm and von Barth have shown that the one-shot and fully self-consistent GWA produce only modest improvement in the local structure of $g(r)$ over the RPA, for the metallic density $r_s = 4$. [35]

As mentioned above, the focus on static properties partly justified ignoring the frequency dependence of the optimized potentials, u_{ij} . However, the structure of the multi-component theory is such that when mapped to the one-component form for $\chi(k, \omega)$, Eq.(II.9), the local field factor G_+ that arises is frequency dependent. It is interesting then to examine theoretical predictions for a dynamic property of the gas: its collective excitations, i.e., plasmons.[6, 19]

Figure 2 shows the plasmon frequency ω_p as a function of wavevector k for various theories and simulation data for the same densities as given in Figure 1. As shown, the plasmon frequency is normalized by its value at zero wavenumber: $\omega_p(0) = \sqrt{4\pi ne^2/m}$. The curves terminate at the beginning of the electron-hole continuum of the non-interacting electron gas.[6] The Corradini et al. curves were obtained using their fit[6, 37] of $G_+(k, 0)$ to QMC simulation data of Moroni et al.[38] for $r_s = 2, 5$ and 10. While not shown in the figure, the predictions of the theory of UI[31] for $r_s = 2$ are essentially the same as those shown for Corradini et al. As can be seen, the RO-RPA predicts larger plasmon frequencies than the STLS theory for all densities, with the difference increasing somewhat as r_s increases. The RO-RPA predictions agree well with the results using the Corradini et al. fit for both densities, $r_s = 2$ and 10. It has been shown elsewhere that the fully self-consistent GWA gives poor predictions for the spectral properties of jellium, including the plasmon modes.[14]

Figure 3 shows theoretical predictions for the scaled correlation energy per particle, ϵ_c , as a function of the scaled average electron separation, r_s . Also shown are simulation data of Ortiz et al.[39], and the Perdew-Wang fit[29] to simulation data of Ceperley and Alder[33]. Vosko et al.[20] show results for ϵ_c for other theories for the paramagnetic phase. As can be seen, the predictions of the RO-RPA greatly improve upon those of the RPA. As mentioned above, the density range of most metals is $2 \leq r_s \leq 6$. [40] For this range, the RO-RPA values for ϵ_c are more negative than those of simulation by 15% on

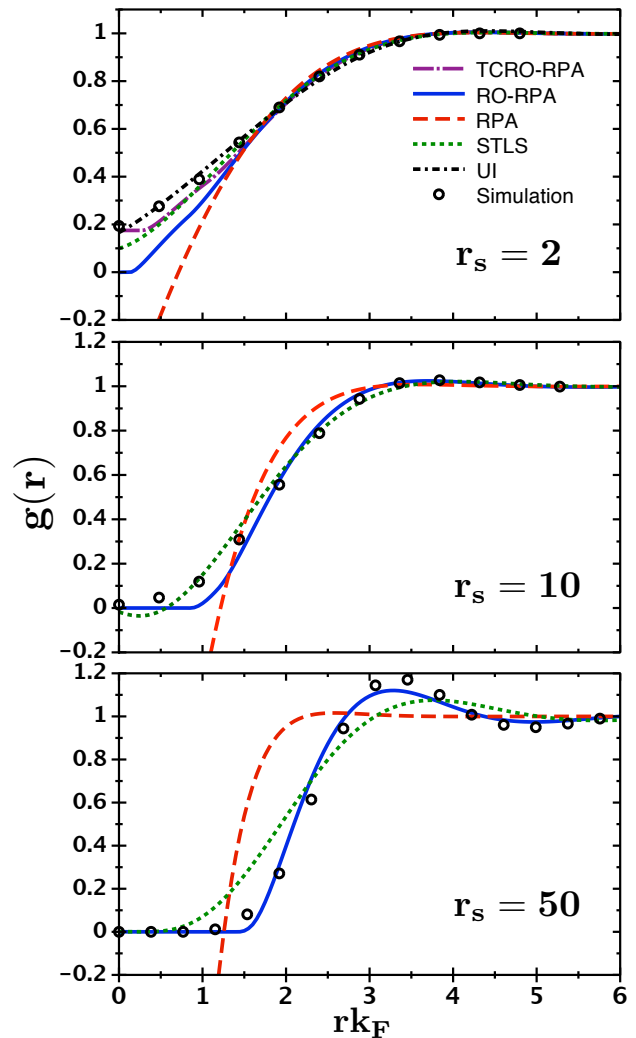


FIG. 1. Spin-averaged pair correlation function $g(r)$ as a function of distance r for various densities. The meanings of the curves and symbols are shown in the figure legend. For $r_s = 2$ and 10, the simulation data are from Ceperley and Alder[33] as obtained from Gori-Giorgi et al.[36] For $r_s = 50$, the simulation data are from Zong et al.[34] The contact value $g(0)$ from the RPA theory is -0.66 , -3.95 and -15.1 for $r_s = 2$, 10 and 50, respectively.

average, while the RPA values are more negative by 46% on average. The accuracy of the RO-RPA increases with decreasing density such that, for example, at $r_s = 40$, its value for ϵ_c is within 3% of simulation. The thermodynamically consistent theory, TCRO-RPA, improves even more on the RPA: its predictions for ϵ_c are within 4% of simulation over the metallic density range. Interestingly, the predictions of the *one*-component RO-RPA theory, while being inferior to the multi-component theory for almost every other quantity, are slightly better than the multi-component for ϵ_c when thermodynamic consistency is enforced. The one-component TCRO-RPA theory agrees with the Perdew-Wang fit to within 3% for the metallic density range. This accuracy is the same or only

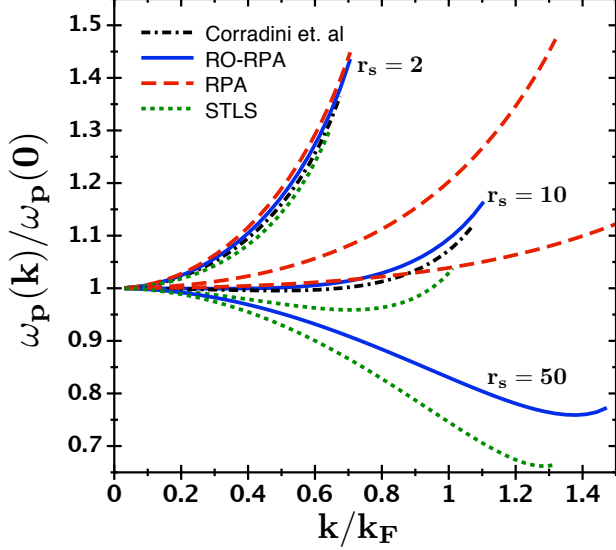


FIG. 2. Plasmon dispersion curves for various scaled average electron separations r_s . The meanings of the curves are shown in the figure legend. An r_s label refers to the closest RO-RPA curve. For the other theories, the trend is for the slope of $\omega_p(k)$ at small k to decrease as r_s increases. The complete RPA curve for $r_s = 50$ is not shown, it terminating with value $\omega_p(k)/\omega_p(0) = 1.55$ at $k/k_F = 2.36$. The Corradini et al. curves were obtained using their fit[37] of $G_+(k, 0)$ to simulation data[38].

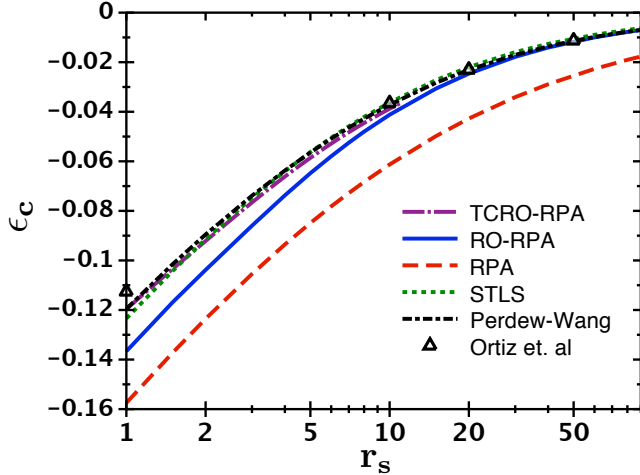


FIG. 3. Scaled correlation energy per particle ϵ_c (in Rydbergs) as a function of the scaled average electron separation r_s . The meanings of the curves and symbols are shown in the figure legend. The Perdew-Wang curve is a fit [29] to simulation data [33].

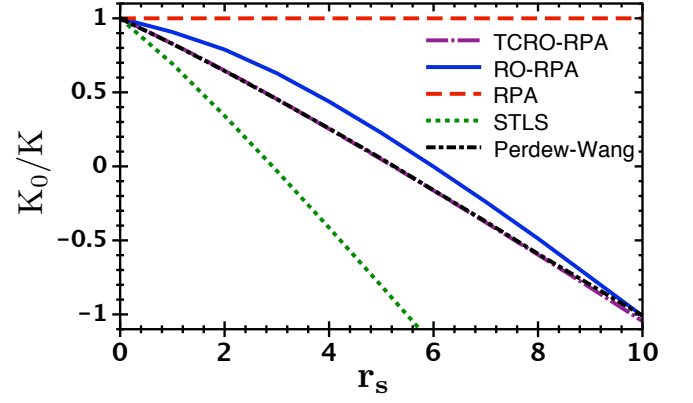


FIG. 4. Scaled inverse compressibility K_0/K as a function of the scaled average electron separation r_s , obtained using Eq.(II.3). The meanings of the curves are shown in the figure legend. Note that the TCRO-RPA and Perdew-Wang curves overlap for almost all densities shown.

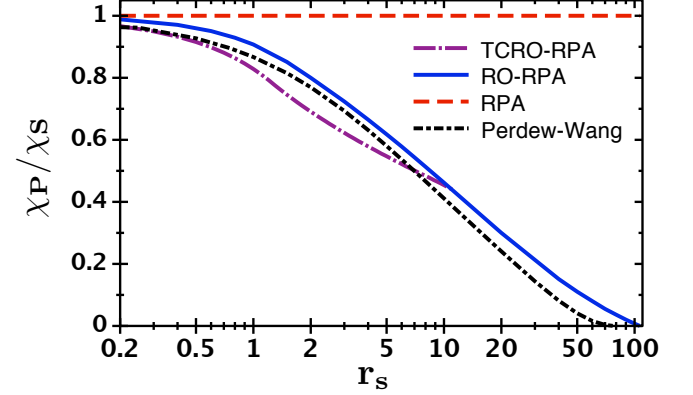


FIG. 5. Scaled inverse spin susceptibility χ_P/χ_S as a function of the scaled average electron separation r_s , obtained using Eq.(II.4). The meanings of the curves are shown in the figure legend.

slightly less than that of the most accurate theories for ϵ_c : STLS,[30] and Vashishta and Singwi,[41] which agree with simulation within 2% and 3%, respectively, over this density range (the UI theory agrees within 7%[31]). While it has been tested to date for only a few densities, the fully self-consistent GWA gives very good agreement for ϵ_c , within 1% for $r_s = 2$ and 4.[14] Given the mediocre predictions of the theory for other properties, this good agreement is thought to be due to a large cancellation of effects.[35]

Figure 4 shows results for the scaled inverse of the compressibility, K_0/K , as defined by the structure equation, Eq.(II.3) above. Simulation values were obtained using the Perdew-Wang fit[29] to data of Ceperley and Alder[33] for the correlation energy, and an expression relating the compressibility to the total energy[6]. For jellium, simulation studies[33] show that the inverse compressibility goes to zero at $r_s = 5.25$. The RO-RPA pre-

dicts a zero at $r_s = 6$, which is 14% higher. As a comparison, the STLS theory predicts a zero at $r_s = 3$, which is 55% less than simulation. As is well known, the RPA gives the non-interacting value at all densities. Interestingly, the TCRO-RPA predictions agree very well with the Perdew-Wang fitted data, within 0.1%, up to $r_s = 8$.

Figure 5 shows results for the scaled inverse of the spin susceptibility, χ_P/χ_S , as defined by the structure equation, Eq.(II.4) above. As for K , simulation values were obtained using the Perdew-Wang fit[29] for the correlation energy, and an expression relating χ_S to the total energy[6]. A divergence in χ_S is identified with a second-order transition from the paramagnetic state to a polarized state. In Hartree-Fock theory, this polarized state was identified with the fully polarized, i.e., ferromagnetic, state.[19] Simulation work appeared to have reinforced this idea.[33] In the Hartree-Fock and RPA theories, the density of the divergence of χ_S is slightly lower (higher r_s) than the density for paramagnetic-ferromagnetic phase coexistence. In their fit then, Perdew and Wang reasoned that the true density of divergence occurs at an r_s slightly above that for paramagnetic-ferromagnetic coexistence, $r_s = 73$, which was computed via simulation by Ceperley and Alder.[33] This reasoning yielded a divergence of χ_S at $r_s = 77.5$. This zero of $1/\chi_S$ can be seen in Figure 5.

Subsequent simulation work by Ortiz et al. found that partially polarized states were energetically favorable at higher densities (lower r_s), and the transition from the paramagnetic to a partially polarized state was continuous.[39] Later simulation work by Zong et al. underscored this picture, though their estimate of the density of this transition was lower, $r_s \approx 50$. [34] In addition, Zong et al. estimated the transition to the ferromagnetic state was at $r_s \approx 100$, which was also their estimate for the transition to the Wigner solid state.[34]

As can be seen in Figure 5, the RO-RPA predicts a divergence at $r_s \approx 107$, in good agreement with the estimate of Zong et al. for the paramagnetic-ferromagnetic transition. So, either the RO-RPA overestimates the value of r_s for the paramagnetic-partially polarized transition by a factor of two, or predicts that only the paramagnetic-ferromagnetic transition is second order. Given the accuracy of the RO-RPA for the correlation energy at low density, the latter explanation appears more plausible. However, the RO-RPA value for the density of divergence was obtained from the structure route expression for the susceptibility, and usually estimates using the energy route are more accurate. Given the form of the RO-RPA multi-component theory, it is straightforward to generalize it to compute E_{corr} as a function of the fractional spin polarization, $p \equiv \langle n_\uparrow(x) - n_\downarrow(x) \rangle / n$, and thus determine coexistence and spinodal boundaries. The solution to this puzzle then is left to future research.

In this work, thermodynamic consistency was enforced on the compressibility, which is a measure of the sensitivity of the electron density to changes in the pressure. It is not expected then that this method would neces-

sarily improve the predictions of the theory for the spin susceptibility, which is a measure of the sensitivity of a different quantity, the spin polarization, to changes in the magnetic field. Nonetheless, it is interesting to examine the TCRO-RPA predictions for χ_S . As can be seen in Figure 5, the TCRO-RPA values agree well with the Perdew-Wang fit at very high density (small r_s), but drop below the Perdew-Wang curve at $r_s \approx 0.5$. For example, at $r_s = 2$, the TCRO-RPA value is 10% below the Perdew-Wang one. For $r_s > 2$, the TCRO-RPA curve asymptotically approaches the RO-RPA curve, terminating at it at $r_s \approx 10.8$. At that point, the TCRO-RPA curve is above the Perdew-Wang curve. In other words, the agreement with the fitted simulation data appears to be better for the RO-RPA than for the TCRO-RPA. It has been remarked elsewhere that the Perdew-Wang fit is not that accurate for polarized states.[6] It seems unlikely though that this inaccuracy would be that large near $p = 0$. A clarifying task then would be to compute χ_S via the energy route. For this, E_{corr} would be computed for small p and constant r_s , while enforcing thermodynamic consistency on K (or even χ_S).

V. SUMMARY AND DISCUSSION

In summary, the range optimization scheme was applied to the RPA theory for jellium. It was shown that this RO-RPA theory gives greatly improved predictions for the gas properties as shown by its results for the pair correlation function $g(r)$, compressibility K and spin susceptibility χ_S . For the correlation energy, E_{corr} , the theory is most accurate at low densities, but it still gives predictions within 15% of simulation for the density range of most metals, $2 \leq r_s \leq 6$. Enforcing thermodynamic consistency on the compressibility improves the agreement with simulation to within 4% for this density range, while the one-component version of the theory is slightly better at 3%. This agreement is comparable to the most accurate of the previous theories for E_{corr} . [14, 30, 41] Also, the RO-RPA appears to outperform the STLS theory in comparison with simulation data for the plasmon modes and compressibility, and the pair correlation function at low density.

The thermodynamically consistent theory could be further improved by conducting the range optimization to obey the cusp condition on $g(r)$ near $r = 0$. [42] Also, since range optimization can be applied to any theory in which the positivity condition of $g(r)$ is violated, improvements in the accuracy of the basic theory are possible.

One noteworthy result was that the RO-RPA theory predicts a divergence of χ_S at a density that is lower than current estimates for the liquid-solid transition.[6, 34] Thus, no divergence of χ_S is predicted for the liquid phase. This result was obtained using the structure route expression for χ_S , Eq.(II.4). Given the evidence from simulations for a transition to partially polarized

states,[34, 39] it would be interesting within the RO-RPA to examine the phase behavior of jellium as a function of polarization using the energy route.[21] Further, since the temperature dependent density-density response function can be represented by an equation almost identical to Eq.(II.7),[19] the full temperature dependent phase diagram can be obtained.

As stated above, one aim of this work is to apply range optimization to inhomogeneous electron liquids, to compute the band structure of semiconductors, for example.

It was shown in Sec.III how the new algorithm to implement range optimization can be applied to inhomogeneous liquids, and results for that will be presented in a future work.

ACKNOWLEDGMENTS

I thank Craig Pryor for helpful conversations.

-
- [1] W. Kohn, Rev. Mod. Phys. **71**, 1253 (1999).
 - [2] J. P. Perdew and S. Kurth, “Density functionals for non-relativistic coulomb systems in the new century,” in *A Primer in Density Functional Theory*, edited by C. Filolhais, F. Nogueira, and M. Marques (Springer-Verlag, Berlin, DE, 2003) p. 1.
 - [3] K. Capelle, arXiv.org (2006), <http://arxiv.org/abs/cond-mat/0211443>.
 - [4] L. Hedin, Phys. Rev. **139**, A796 (1965).
 - [5] W. G. Aulbur, L. Jönsson, and J. W. Wilkins, Solid State Physics **54**, 1 (2000).
 - [6] G. F. Giuliani and G. Vignale, *Quantum Theory of the Electron Liquid* (Cambridge University Press, New York, NY, USA, 2005).
 - [7] V. D. Gorobchenko, V. N. Kohn, and E. G. Maksimov, “The dielectric function of the homogeneous electron gas,” in *Modern Problems in Condensed Matter Sciences, Vol. 24: The Dielectric Function of Condensed Systems*, edited by L. V. Keldysh, D. A. Kirzhnits, and A. A. Maradudin (Elsevier Science Publishers B.V., Amsterdam, NL, 1989) p. 87.
 - [8] J. G. Angyan, R.-F. Liu, J. Toulouse, and G. Jansen, J. Chem. Theory Comput. **7**, 3116 (2011), and references therein.
 - [9] Y. M. Niquet and X. Gonze, Phys. Rev. B **70**, 245115 (2004).
 - [10] J. Toulouse, I. C. Gerber, G. Jansen, A. Savin, and J. G. Angyan, Phys. Rev. Lett. **102**, 096404 (2009).
 - [11] J. Klimes and A. Michaelides, J. Chem. Phys. **137**, 120901 (2012).
 - [12] F. Bruneval, N. Vast, and L. Reining, Phys. Rev. B **74**, 045102 (2006).
 - [13] P. Yu and M. Cardona, *Fundamentals of Semiconductors: Physics and Material Properties* (Springer-Verlag, Berlin, DE, 2010).
 - [14] B. Holm and U. von Barth, Phys. Rev. B **57**, 2108 (1998).
 - [15] J. P. Donley, D. R. Heine, and D. T. Wu, Phys. Rev. E **70**, 060201 (2004).
 - [16] J. P. Donley, D. R. Heine, and D. T. Wu, Macromolecules **38**, 1007 (2005).
 - [17] J. P. Donley and D. R. Heine, Macromolecules **39**, 8467 (2006).
 - [18] J. P. Donley, D. R. Heine, C. A. Tormey, and D. T. Wu, J. Chem. Phys. **141**, 024504 (2014).
 - [19] A. L. Fetter and J. D. Walecka, *Quantum Theory of Many-Particle Systems* (Dover Publications, Mineola, NY, USA, 2003).
 - [20] S. H. Vosko, L. Wilk, and M. Nusair, Can. J. Phys. **58**, 1200 (1980).
 - [21] S. Tanaka and S. Ichimaru, Phys. Rev. B **39**, 1036 (1989).
 - [22] J. P. Hansen and I. R. McDonald, *Theory of Simple Liquids* (Academic Press, London, UK, 1986).
 - [23] J. L. Lebowitz and J. K. Percus, Phys. Rev. **144**, 251 (1966).
 - [24] R. Dickman and G. Stell, Phys. Rev. Lett. **77**, 996 (1996).
 - [25] D. Pines and P. Nozieres, *Theory of Quantum Liquids* (Westview Press, Boulder, CO, USA, 1999).
 - [26] W. H. Press, S. A. Teukolsky, W. T. Vetterling, and B. P. Flannery, *Numerical Recipes in C: The Art of Scientific Computing* (Cambridge University Press, New York, NY, USA, 1992).
 - [27] The RPA values for the spin-averaged $g(0)$ agree best with those of Toigo and Woodruff[43] and Gorobchenko et al.[7].
 - [28] R. M. Martin, *Electronic Structure: Basic Theory and Practical Methods* (Cambridge University Press, New York, NY, USA, 2004).
 - [29] J. P. Perdew and Y. Wang, Phys. Rev. B **45**, 13244 (1992).
 - [30] K. S. Singwi, M. P. Tosi, R. H. Land, and A. Sjölander, Phys. Rev. **176**, 589 (1968).
 - [31] K. Utsumi and S. Ichimaru, Phys. Rev. B **22**, 5203 (1980).
 - [32] T. Gould and J. F. Dobson, Phys. Rev. A **85**, 062504 (2012).
 - [33] D. M. Ceperley and B. J. Alder, Phys. Rev. Lett. **45**, 566 (1980).
 - [34] F. H. Zong, C. Lin, and D. M. Ceperley, Phys. Rev. E **66**, 036703 (2002).
 - [35] B. Holm and U. von Barth, Physica Scripta **T109**, 135 (2004).
 - [36] P. Gori-Giorgi, F. Sacchetti, and G. B. Bachelet, Phys. Rev. B **61**, 7353 (2000).
 - [37] M. Corradini, R. Del Sole, G. Onida, and M. Palumbo, Phys. Rev. B **57**, 14569 (1998).
 - [38] S. Moroni, D. M. Ceperley, and G. Senatore, Phys. Rev. Lett. **75**, 689 (1995).
 - [39] G. Ortiz, M. Harris, and P. Ballone, Phys. Rev. Lett. **82**, 5317 (1999).
 - [40] N. W. Ashcroft and N. D. Mermin, *Solid State Physics* (Saunders College, Philadelphia, PA, USA, 1976).
 - [41] P. Vashishta and K. S. Singwi, Phys. Rev. B **6**, 875 (1972).
 - [42] J. C. Kimball, Phys. Rev. A **7**, 1648 (1973).
 - [43] F. Toigo and T. O. Woodruff, Phys. Rev. B **4**, 371 (1971).